Optimization of austenitic and ferritic steels for deep drawing. Part 1: metallurgical and mechanical analyses.

Andrea Casaroli, Edoardo Scabini, Marco V. Boniardi, Riccardo Gerosa, Barbara Rivolta
Department of Mechanical Engineering, Politecnico di Milano, via La Masa 1, 20156 Milano, Italy
andrea.casaroli@polimi.it , https://orcid.org/0000-0001-5207-5547
edoardo.scabini@polimi.it , https://orcid.org/0009-0005-4487-912X
marco.boniardi@polimi.it , https://orcid.org/0000-0002-2438-7890
riccardo.gerosa@polimi.it , https://orcid.org/0000-0003-0810-0279
barbara.rivolta@polimi.it , https://orcid.org/0000-0002-8949-0549

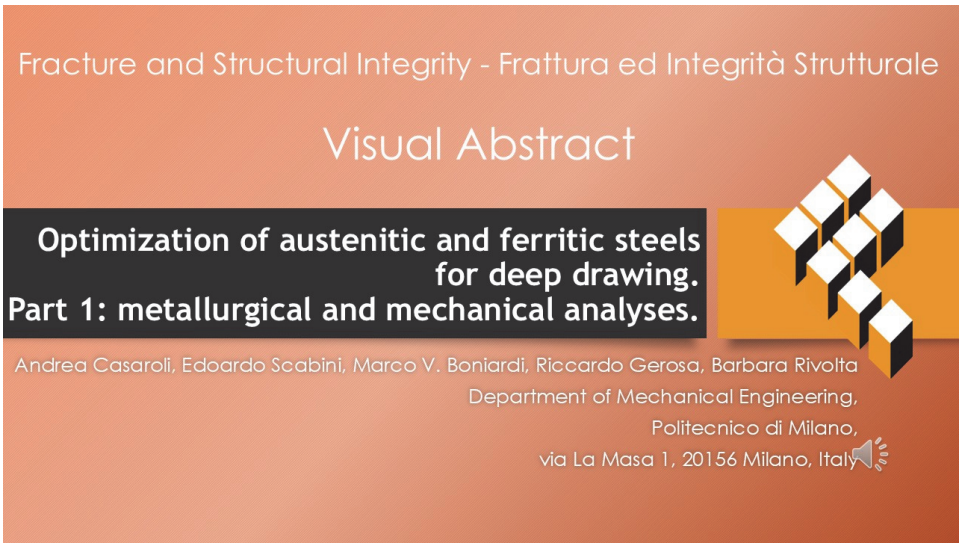

Citation: Casaroli, A., Scabini, E., Boniardi, M. V., Gerosa, R., Rivolta., B., Optimization of austenitic and ferritic steels for deep drawing. Part 1: metallurgical and mechanical analyses., Fracture and Structural Integrity, 75 (2026) 104-123.

Received: 25.09.2025
Accepted: 15.10.2025
Published: 18.10.2025
Issue: 01.2026

KEYWORDS. Deep drawing, Stainless steels, Process parameters, Lubrication analyses, Erichsen test, metallographic analyses, ANOVA.

INTRODUCTION

The deep drawing process of stainless steel sheet metal represents a fundamental technology for modern industry, thanks to its ability to generate a wide range of high quality and low cost products for applications in the food industry [1,2] for nautical equipment, for applications in the chemical or petrochemical sector which must guarantee high resistance to corrosion, for design objects and more generally for high added value uses in the civil and industrial sectors. The possibility of rapid mass production, combined with the ability to minimize waste, make deep drawing a highly competitive manufacturing method in terms of costs per unit produced.

Despite its apparent simplicity, the process presents numerous critical issues, related both to the properties of the stainless steel and to the processing parameters, which can generate different types of defects, such as wrinkles, scratches and bottom breaks.

To improve the process, it is possible to work on different operating conditions such as, for example, the force of the blank-holder, the lubrication mode and the deformation speed, which influence the ability of the sheet metal to adapt to the desired profile [3]. Specifically, the pressure of the blank-holder must avoid the creation of wrinkles during processing, but must still allow the flow of material so that areas with excessive reduction in thickness are not generated. Lubrication, which can occur with the application of plastic films or liquid lubricants of different nature, is very important for several factors [4], briefly summarized below.

- It reduces the wear of the equipment used for deep drawing, which represents one of the most important problems. The degradation is mainly due to adhesive wear phenomena that cause the creation of scratches and surface grooves [5] from which, over time, the loss of geometric and dimensional tolerances of the die occurs. This problem is strongly influenced by the friction coefficient between the die and the sheet metal: the greater the friction, the greater the adhesion phenomenon and therefore the wear.
- It promotes the relative sliding of the stainless steel with respect to the punch, making the distribution of the stresses and the corresponding deformations uniform within the sheet metal.
- Increases the overall process efficiency by reducing the forces applied to the die.

One of the main deep drawing problems is related to the ability of a liquid lubricant to remain in the contact area between the die and the sheet metal during the deformation process.

This shaping process always produce a sliding between the parts in contact, which results in a shear stress in the lubricant. In the case of liquid lubrication, these conditions induce a leak of the lubricant from the working area and, in extreme cases, it can be completely expelled generating local dry sliding conditions [6]. This problem can be increased further by the die geometry. Unfortunately, the great number of factors that influence the lubricant properties such as, the chemical composition, its viscosity [7] and its sensitivity to the temperature and the pressure, make the modelling of the contact area extremely complex. It is hence often necessary to investigate the influence of the lubricant by expensive experimental campaigns.

The strain rate also influences the behaviour of stainless steel sheets [8–10] subjected to deep drawing. The constitutive law, used to describe the stress of a generic metallic material subjected to deformation, models the effect of the strain and the strain rate through the exponents n and m as reported in Eqn. (1):

$$\sigma^* = C \cdot \varepsilon^{*n} \cdot \dot{\varepsilon}^{*m} \tag{1}$$

where:

- σ^* represents the true stress experienced by the material, calculated as $\sigma^* = \sigma \cdot (\varepsilon + 1)$
- σ and ε are the engineering stress and strain, respectively.
- C is the strain hardening coefficient of the material.
- ε^* e $\dot{\varepsilon}^*$ represent the true strain and the true strain rate calculated as, $\varepsilon^* = \ln(1+\varepsilon)$ and $\dot{\varepsilon}^* = \frac{d\varepsilon^*}{dt}$ time derivative of the true strain.
- n represents the strain hardening exponent of the material.
- m represents the strain rate sensitivity.

As the strain rate increases, a generic metallic material undergoes an increase in mechanical strength at the expense of deformability. Excessively high die speeds, cause therefore a decrease in the sheet metal deformation capacity, increasing both the forces and the defectiveness of the component [11]. To evaluate the deformability of the sheet metal subjected to deep drawing conditions, tests such as the Erichsen or the Ball Punch ones have been designed. These tests, whose execution methods are defined by the standards EN ISO 20482 and ASTM E643, are performed by imposing the movement of a hemispherical punch in a perpendicular direction to a sheet metal blocked by a blank-holder. The Erichsen testing machine is shown in Figure 1. The test result is expressed by the depth of the cup created at the time of failure, defined as the Erichsen index IE.

If the geometry is so complex that it prevents the component from forming, different strategies can be adopted such as, for example, increasing the number of steps the total deformation is obtained with, use intermediate heat treatments such as recrystallization annealing, choose the right microstructural condition before forming and improving the geometry of the part in order to adapt the deformation mode to the mechanical and metallurgical properties of the employed stainless steel.

The main heat treatments carried out on stainless steels subjected to deep drawing are solution annealing and full annealing, since they can maximize the material deformability

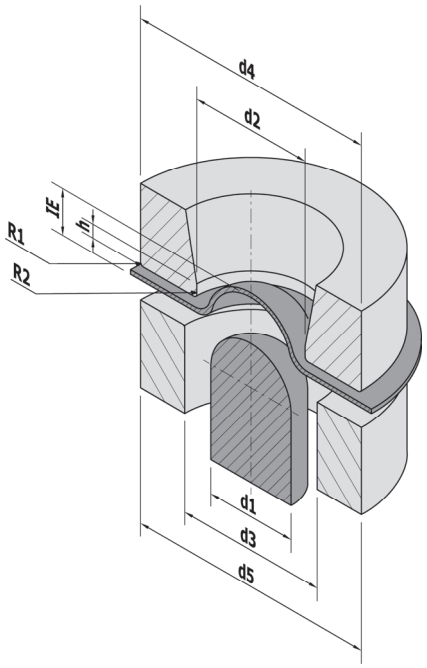

Figure 1: Section of a generical Erichsen testing machine. d_1 is the diameter of the punch, while d_2 and d_3 represent the internal diameter of the die and the blank holder. r_2 is the internal radius of the blank-holder. The result of the test is represented by the depth of the spherical cup (IE).

Solution annealing is performed on both semi-finished and finished products made with austenitic stainless steel. The heat treatment is carried out at high temperature (approximately between 1000°C and 1100°C), for a time that guarantees the homogenization of the chemical composition of the steel: during the treatment, any microstructural heterogeneity is eliminated, especially chromium carbides and sigma phase. To ensure successful heat treatment, austenitic stainless steels must be rapidly quenched in water, especially for thick components. Cooling must be rapid to avoid the precipitation of carbides at the grain boundaries between 450 °C and 900 °C. In the case of thin thickness, a high-pressure nitrogen flow can be used.

Full annealing, performed on ferritic stainless steels, is carried out at different temperatures based on the chemical composition (generally between 770 °C and 930 °C). It is important to pay great attention to temperature and the holding time, since this family of stainless steel is very sensitive to grain growth. The cooling phase is performed in air for thin-walled semi-finished products or for long semi-finished products with a small diameter; in water for components with a larger section.

During both the solution and the full annealing, recrystallization may take place: after a cold plastic deformation, in fact, new polygonal grains are generated starting from the original deformed microstructure. Regarding austenitic stainless steels, when a large plastic deformation is applied, local formation of martensite may occur [12], changing the material behavior significantly, possibly making the used process parameters not optimal for the new microstructural condition. The structural stability under plastic deformation can often be evaluated by means of coefficients such as the M_{d30}, that represents the temperature at which martensite can be formed from austenite under a deformation of 30%. The M_{d30} value can be related to the chemical composition by different formulas present in the technical literature. In particular, Nohara et al. [13] proposed Eqn. (2) including the influence of the grain size as well:

$$M_{d30}\,[°C] = 551 - 462\cdot(C+N) - 9.2\cdot Si - 8.1\cdot Mn - 13.7\cdot Cr - 29\cdot Ni - 18.3\cdot Mo - 29\cdot Cu - 68\cdot Nb - 1.42\cdot(\text{ASTM grain size number} - 8) \quad (2)$$

In the previous formula, all the chemical elements content is in wt%. When the M_{d30} value decreases (i.e. the temperature becomes colder), the austenite stability increases making the selected deep drawing parameters optimal also for large

deformations. Eqn. (2) remarks the importance of the chemical composition, but highlights the role of the grain size too. The use of heat treatments is hence not only critical from economic point of view, as it increases production times and requires significant changes to the plant, but can have a detrimental effect because of the grain coarsening. In order to improve the deep drawability of stainless steels, grades with a special chemical composition have been developed. One of the most widely used austenitic stainless steel type is AISI 304, of which there is a modified version dedicated to deep drawing, called 304 mod. from here on. This material is characterized by a lower chromium content and a higher nickel amount, in order to stabilize the austenite and reduce the possibility of its transformation into martensite through plastic deformation [14] in agreement with Eqn. (2). Among the ferritic stainless steels, AISI 441 is considered more suitable for deep drawing in respect to AISI 430. AISI 441 is characterized by a very limited carbon content and the presence of small amount of titanium and niobium to stabilize the ferrite and prevent the precipitation of chromium carbides [15].
This research paper aims to study the differences among standard and deep drawing-optimized austenitic and ferritic stainless steels. Moreover, the deep drawability of the two stainless steel types will be compared with their own deformation capacity, evaluated by means of the percentage elongation at fracture. Then, considering the cost of ferritic stainless steels, significantly lower than that of austenitic grades, the results of the experimental tests will be evaluated considering this aspect too. In addition to the different steel types, the effect of the deformation rate, the type of lubrication and the blank-holder pressure was also considered. The stainless steels were fully characterized by tensile, Erichsen and HV0.2 microhardness tests and by micrographic analyses, aimed to understand the metallurgical properties of the steel varying the process parameters. The experimental plan was designed following the rules defined by the Design of Experiment (DoE) and the results were statistically analysed by the ANOVA technique in order to maximize the effectiveness of the experiment.

DEFORMATION MODES IN DEEP DRAWING PROCESSES

The deep drawing process causes a strong plastic deformation in the material in three dimensions. During a plastic deformation, the volume is constant and consequently the sum of the three principal strains is equal to zero as reported in Eqn. (3) [16].

$$\varepsilon_l+\varepsilon_w+\varepsilon_t=0 \tag{3}$$

where ε_l, ε_w, ε_t are the strains in the longitudinal, long transverse and short transverse (thickness) directions respectively.
Considering the strains occurring on thin metal sheets, Figure 2 shows two main types of deformation:

- drawing: the deformation is positive in one direction, while in the transverse direction negative strain occurs. This type of deformation is characteristic of processes in which the material is stretched predominantly in one direction, while the others are reduced. A typical example of this phenomenon is observed in the tensile test. In the deep drawing process, this deformation occurs in the steel flowing under the blank-holder.
- stretching: the strain is positive both in the longitudinal and transverse directions. This condition, typical of the area of the sheet metal in contact with the die, is more severe than drawing because it requires a significant reduction in thickness to maintain the volume constant.

By relating the deformations that occur on the plane of the sheet metal, it is possible to create a graph that describes the two modes previously exposed. The bisector of the first quadrant shows a particular deformation mode, called balanced biaxial, in which the planar deformation occurs in both directions in an equivalent way.
Figure 3 shows a deformability limit curve, which is a useful tool to determine the maximum deformation applicable in the plane before the steel breaks [17]. This curve can be obtained experimentally, through ad hoc tests, or analytically, using for example the Storen-Rice model [18]; a third possibility is the numerical one, through the use of finite element models. The FLD curve is influenced by the material strain hardening exponent, by the sheet thickness and by the strain rate [19]: when the strain hardening exponent and the thickness increase and when the strain rate decreases, the FLD curves shift upward enlarging the safe zone. For a fixed sheet thickness and deformation rate, the ferritic stainless steels are hence disadvantaged being their strain hardening exponent generally lower than austenitic grades.
The deformability limit curve is particularly useful for deep drawing processes, because it allows to predict any possible critical issues [20]. Considering the Erichsen test instead, it is easy to understand how the spherical shape of the punch imposes stretching conditions in the sheet metal between the punch and the blank-holder; the deformation is instead balanced biaxially at the apex of the cup. The deformability limit curve also allows to understand that the deformation conditions imposed by the Erichsen test are less severe than the plane strain condition in which the deformation is blocked in the direction perpendicular to the force [21].

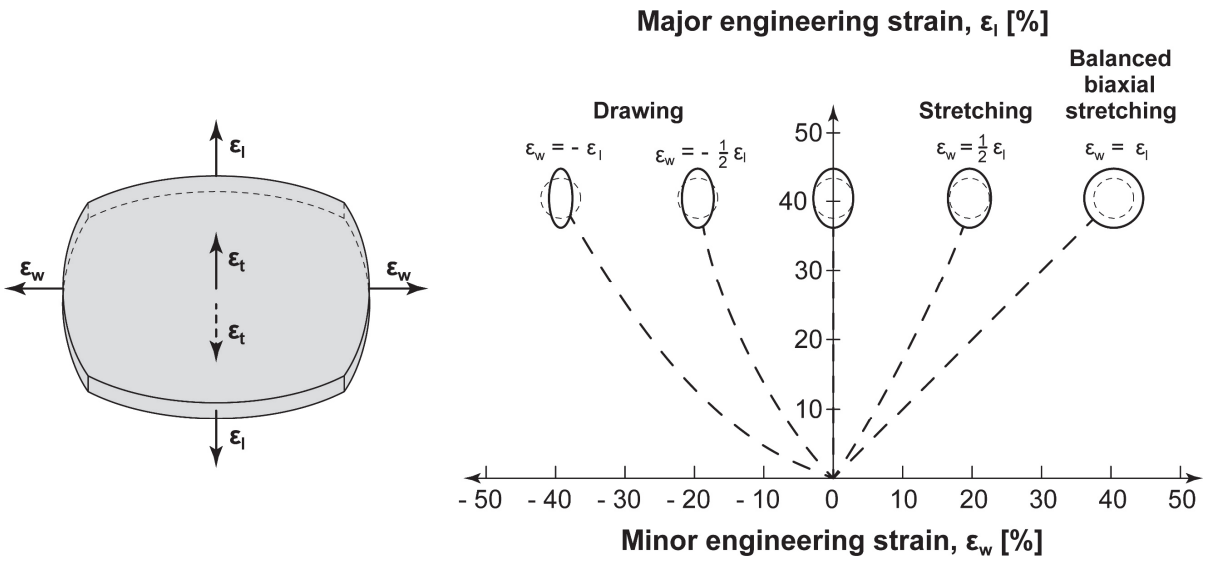

Figure 2: Deformation modes based on planar deformation values. The major and minor deformation are those on sheet metal plane expressed by ε_l and ε_w. In the left area the deformation occurs by drawing while in the right one by stretching.

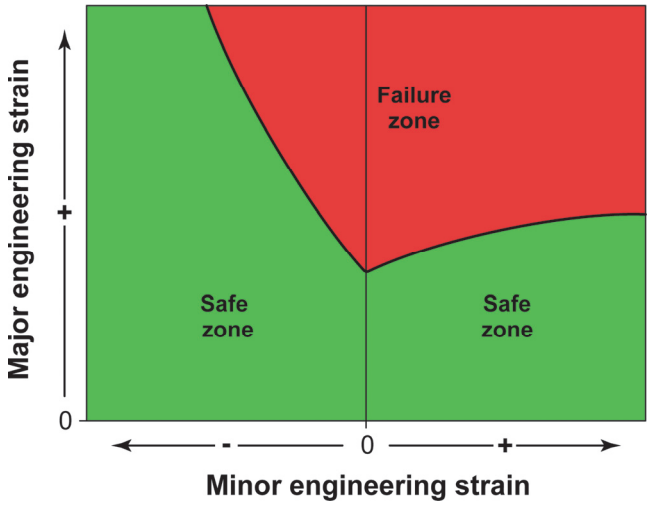

Figure 3: Generical example of a deformability limit curve. The image shows how the limit curve for drawing, in the left area, allows larger deformations than the one for stretching, in the right area.

MATERIALS AND METHOD

The materials under investigation are two austenitic and two ferritic stainless steels, designated according to the ASTM A240/240M standard. For both, two grades commonly used in the industry were considered (AISI 304 and AISI 430). Moreover, other two steels were considered because of their improved formability (304 mod. and AISI 441). The chemical compositions are reported in Table 1.

The four steels, produced in the form of 1 mm thick sheet metal, were supplied in condition 2B, i.e. full annealed for ferritic and solubilized for austenitic, pickled and skin passed.

The experimental plan involved mechanical, technological and metallographic tests and analyses. The materials properties were first investigated by uniaxial tensile tests. Then, Erichsen tests were performed to study statistically significant differences between standard grades and those with improved formability. The influence of the lubricant type, of the punch speed and of the blank-holder pressure was also considered. Finally, a wide metallographic analysis and Vickers HV0.2 microhardness tests were carried out along the sheet metal profile at the end of the Erichsen test, in order to highlight the local microstructural and mechanical modifications induced by the deformation process varying the test parameters.

[%]	C	Cr	Ni	Mn	Si	S	P	Cu	Mo	Ti	Nb	N
AISI 304	0.04	18.05	8.02	1.72	0.37	<0.01	0.04	0.04	0.21	-	0.03	0.06
ASTM A240: AISI 304	<0.08	18-20	8-11	<2.00	<0.75	<0.03	<0.045	-	-	-	-	<0.10
304 mod.	0.05	18.06	9.56	1.46	0.35	<0.01	0.03	0.03	0.15	-	0.03	0.03
Limit values for 304 mod.	<0.05	18-18.75	9-10.50	<2.00	<0.75	-	-	-	-	-	-	-
AISI 430	0.05	16.19	0.55	0.47	0.33	<0.01	0.04	0.04	0.02	-	0.03	0.05
ASTM A240: AISI 430	<0.12	16-18	<0.75	<1.00	<1.00	<0.03	<0.04	-	-	-	-	-
AISI 441	0.03	17.87	0.4	0.33	0.58	<0.01	0.04	0.04	0.04	0.25	0.45	0.01
ASTM A240: AISI 441	<0.03	17.5-19.5	<1.00	<1.00	<1.00	<0.03	<0.04	-	-	0.1-0.5	0.57-0.9	<0.03

Table 1: Experimental chemical composition of the sheets used for the experimentation compared to the limit values. AISI 304 is similar to EN X5CrNi18-10. 304 mod. is characterized by a chemical composition compatible with the AISI 304 limits, compared to which it establishes lower maximum chromium and higher minimum nickel contents. AISI 430, similar to X6Cr17. AISI 441, similar to X2CrTiNb18. AISI 441 is characterized by a very limited carbon content and the addition of small amount of titanium and niobium to stabilize the ferrite and prevent the precipitation of chromium carbides.

Tensile tests

For each type of stainless steel, nine tensile specimens were obtained, three of which were machined parallelly (L), three perpendicular (T) and three at 45° (Q) with respect to the rolling direction. The results, expressed as the mean value of the three replicates, are summarized in Tab.4. Each tensile test was carried out according to the ISO 6892 standard at a deformation rate of 0.005 s^{-1} until the elongation of 2%, then it was increased to 0.05 s^{-1} until failure.

From each test, the values of the yield strength, $R_{p0.2}$, the ultimate tensile strength, R_m, the percentage plastic extension at maximum force, A_g%, and the percentage elongation after fracture, A% (L_0 = 25 mm) were determined. Moreover, the strain hardening exponent was calculated according to ISO 10275, in the engineering strain range 4%-15%, while the strain ratio was estimated according to ISO 10113, using the slope, m_r, of the true plastic width strain vs. true plastic length strain line. The true plastic width strain, ε_b, and the true plastic length strain, ε_l, were measured at the engineering strains of 2%, 4%, 8% and 12%. Then, from the r values measured in the three investigated directions the normal ($\bar{r}$) and the planar anisotropy (Δr) coefficients were obtained. The strain ratio value is defined by Eqn. (3), whereas the normal and the planar anisotropy coefficients were determined according to Eqns. (4) and (5).

$$r_{0\text{-}90\text{-}45} = -\frac{m_{r,\ 0\text{-}90\text{-}45}}{1+m_{r,\ 0\text{-}90\text{-}45}} \tag{3}$$

$$r_{0\text{-}90\text{-}45} = -\frac{m_{r,\ 0\text{-}90\text{-}45}}{1+m_{r,\ 0\text{-}90\text{-}45}} \tag{4}$$

$$r_{0\text{-}90\text{-}45} = -\frac{m_{r,\ 0\text{-}90\text{-}45}}{1+m_{r,\ 0\text{-}90\text{-}45}} \tag{5}$$

where $r_{0\text{-}90\text{-}45}$ are the strain ratios in the longitudinal, transversal and 45° directions, $\varepsilon_{w,0\text{-}90\text{-}45}$ and $\varepsilon_{t,0\text{-}90\text{-}45}$ are the strains in the width and the thickness direction for the three specimens series.

Erichsen tests

The Erichsen tests, performed according to EN ISO 20482, were carried out following the experimental setup described in Figure 1 and Table 2.

Description	Symbol [Figure 1]	Dimension [mm]
Punch diameter	d_1	20
Die bore	d_2	27
Blank-holder bore	d_3	33
Outer diameter of the die	d_4	55
Outer diameter of the blank-holder	d_5	55
Outer radius of the die and the blank holder	R_1	0.75

Table 2: Experimental setup used for Erichsen tests.

The considered test conditions regarded the materials, the lubricant type and the lubricated area, the punch speed and the blank-holder pressure. More details are given in Table 3. The lubrication methods were selected to evaluate the effect of both solid lubricants, in the form of PVC adhesive film, and liquid ones, using petroleum jelly. The effect of the lubrication zone was also studied by applying the lubricant in the working area of the blank-holder, on the punch or on a combination of both surfaces. In each case, the lubricant was applied manually, taking care to create a homogeneous layer well adherent to the sheet metal. The experimental plan was set up following the rules of the Design of Experiment for complete and orthogonal planes, replicated three times for a total of 336 tests. The order of execution was completely randomized and the results were statistically analysed according to the ANOVA technique.

Factor	Level		Code
Material	AISI 304		304
	304 mod.		304 mod.
	AISI 430		430
	AISI 441		441
Lubrification	Without lubrication		D
	Petroleum jelly	Blank-holder + Punch	J
		Blank-holder	JH
		Punch	JP
	PVC	Blank-holder + Punch	P
		Blank-holder	PH
		Punch	PP
Punch speed	4.3 mm/min		L
	120 mm/min		H
Blank-holder pressure	6.6 MPa		L
	59.2 MPa		H

Table 3: Factors, factor levels and level coding used for Erichsen tests.

Metallographic analysis and hardness tests

The samples dedicated to the metallographic analysis were mirror polished using abrasive papers with decreasing grit (120, 320, 400, 600, 800, 1200 grit) and cloths with synthetic diamond abrasive (3 μm and 1 μm grit). Lubrication was ensured using water for the papers and the suspension containing the abrasive for the cloths. The etching was carried out chemically using Vilella reagent (hydrochloric acid, 5mL, picric acid, 1g, and ethanol, 100mL), for ferritic stainless steels, and

electrochemically with a solution of 10 g of oxalic acid in 100 mL of distilled water, for austenitic stainless steels. The images were acquired using a LEICA® DM4000M optical microscope. The same samples were also used to evaluate the hardness according to ISO 6507. The tests were performed using a Vickers LEITZ®-WETZLAR® microhardness tester equipped with a digital camera, using the hardness scale HV0.2 (0.2 kg_f, 15 s).

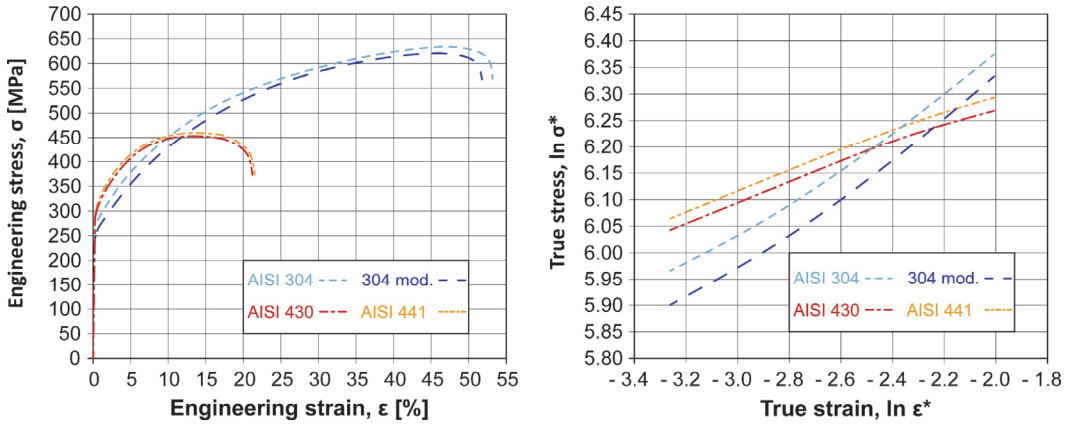

Figure 4: Comparison of engineering stress-strain curves (left) and true stress - true strain regression lines in the 4%-15% strain range (right) for the austenitic stainless steels AISI 304 and 304 mod. and the ferritic stainless steels AISI 430 and AISI 441. Samples are obtained in longitudinal (L) direction.

Material	Direction	$R_{p0.2}$ [MPa]	R_m [MPa]	A%	A_g%	n
AISI 304	Longitudinal L	270	661	53	47	0.343
	Transverse T	267	646	56	48	0.319
	45° Q	263	643	56	48	0.324
304 mod.	Longitudinal L	256	642	51	45	0.360
	Transverse T	260	631	57	48	0.329
	45° Q	269	621	54	47	0.323
AISI 430	Longitudinal L	335	487	22	13	0.188
	Transverse T	343	492	22	13	0.175
	45° Q	341	484	19	12	0.167
AISI 441	Longitudinal L	320	476	22	13	0.190
	Transverse T	335	481	22	13	0.172
	45° Q	329	479	22	13	0.184

Table 4: Experimental results of tensile tests (yield strength, $R_{p0.2}$, ultimate tensile strength, R_m, elongation after fracture, A%, percentage plastic extension at maximum force, A_g% and strain hardening exponent, n) for the austenitic stainless steels AISI 304 and 304 mod. and for the ferritic ones AISI 430 and AISI 441 (right). The specimens are obtained longitudinal, perpendicular and at 45° respect to the rolling direction and each value is expressed as the mean of three replicates.

RESULTS AND DISCUSSION

Tensile tests

Besides the expected differences among the stainless steel grades [22], the tensile tests showed no significant difference among the standard grades (AISI 304 and AISI 441) and those improved for deep drawing (304 mod. and AISI 441). As shown in Figure 4 and Tab. 4, the yield strength of ferritic stainless steels is higher than that of austenitic ones, which however, thanks to their excellent plastic deformability and high work hardening index, have a higher ultimate tensile strength. The plastic deformability of the fcc lattice, typical of austenitic stainless steels, is in fact much higher than that of the bcc lattice. The values of the strain ratio r reported in Table 5, remarks an interesting difference among the ferritic and austenitic stainless steel sheets, being the normal anisotropy

coefficient of the former clearly higher than that of the latter. On the other hand, no notable difference was observed inside each steel type. In this regard, it is interesting to note how austenitic stainless steels behave in an almost isotropic way both along the thickness, with a value of $\bar{r}$ close to 1, and in the different direction on the plane, with a Δr close to zero. On the contrary, ferritic stainless steels show significant anisotropy along all directions.

Material	Direction	r	$\bar{r}$	Δr
AISI 304	Longitudinal L	0.989	1.22	-0.40
	Transverse T	1.054		
	45° Q	1.426		
304 mod.	Longitudinal L	0.796	1.18	-0.39
	Transverse T	1.169		
	45° Q	1.375		
AISI 430	Longitudinal L	1.288	2.42	1.90
	Transverse T	5.458		
	45° Q	1.468		
AISI 441	Longitudinal L	2.236	2.68	0.89
	Transverse T	4.003		
	45° Q	2.231		

Table 5: Experimental results of the strain ratio, r. The values of "r" were also used to evaluate the coefficients $\bar{r}$ and Δr needed to estimate the anisotropy level of the stainless steels. The specimens are obtained in the longitudinal, perpendicular and at 45° respect to the rolling direction.

Erichsen Tests

The large amount of experimental data (336 Erichsen tests) was subjected to ANOVA statistical analysis, with all the interactions between the factors. Graphical analyses of the main effects and their possible interactions are reported in Figure 8 and Figure 9 while the ANOVA table (p-value of 0.05) and the pairwise comparisons according to Tukey's test (p-value of 0.05) up to the second order are reported in Table 6 and Table 7. The assumptions of normality, homoscedasticity and independence [23] were verified for each analysis, without highlighting noteworthy anomalies. Both the preliminary graphic analysis and the ANOVA confirm what was found from the tensile tests: austenitic stainless steels have Erichsen index higher than ferritic ones, while the differences between the standard grades (AISI 304 and AISI 430) and those improved for deep drawing (304 mod. and AISI 441) are limited (on average less than 0.3 IE), despite being statistically different. The pairwise comparison highlights that AISI 441 has a slightly better IE (i.e. slightly higher) than AISI 430 while the 304 mod. does not show any advantages compared to AISI 304 which instead has a slightly higher IE. It is important to underline that the results of the Erichsen test are very influenced by the strain hardening exponent and by the percentage plastic elongation at maximum load, Ag%. High values of such parameters, in fact, have a superior tolerance to local concentration of strain and stress due, for example, to imperfections of the sheet metal, to inhomogeneous lubrication or to geometric errors of the die, avoiding both localized necking phenomena and unwanted breakages during the deep drawing process. Moreover, the major and the minor strains in this kind of test are both positive and stay in the right side of the FLD curve, where the influence of the strain ratio $\bar{r}$ is low. The strain hardening exponent of the ferritic stainless steels is hence a great disadvantage for such kind of plastic deformations as visible in Figure 5. In the technical literature, many authors proposed different approaches to predict the formability curves [19]. The ones presented in Figure 5 is based on the Storen-Rice criterion [24]. According to this approach, the minor and major strains can be calculated according to Eqns. (6) and (7) respectively.

$$\varepsilon_{major} = \frac{3\alpha^2 + n(2+\alpha)^2}{2(2+\alpha)(1+\alpha+\alpha^2)} \tag{6}$$

$$\varepsilon_{minor} = \alpha \varepsilon_{major} \tag{7}$$

where n is the strain hardening exponent and $\alpha = \frac{d\varepsilon_{minor}}{d\varepsilon_{major}}$, $(-1 \leq \alpha \leq 1)$.

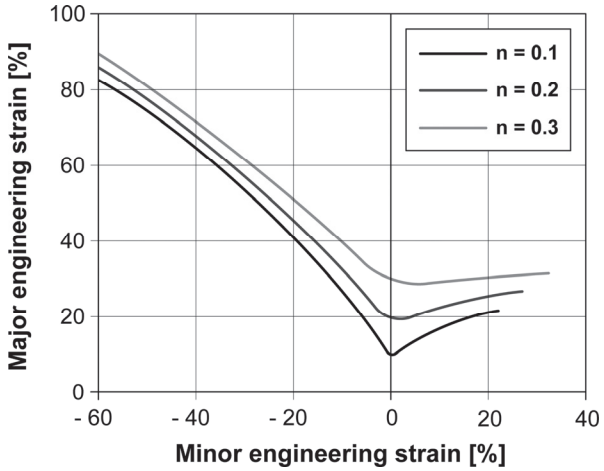

Figure 5: Influence of the strain hardening exponent on the formability limit curves experimentally calculated using formulas number (6) and (7).

In the left side of the FLD curves, where drawing deformation is located, a higher normal anisotropy coefficient is beneficial and can limit the deformability gap with the austenitic grades. Figure 6 shows the influence of such coefficient on the limit major and minor strains.

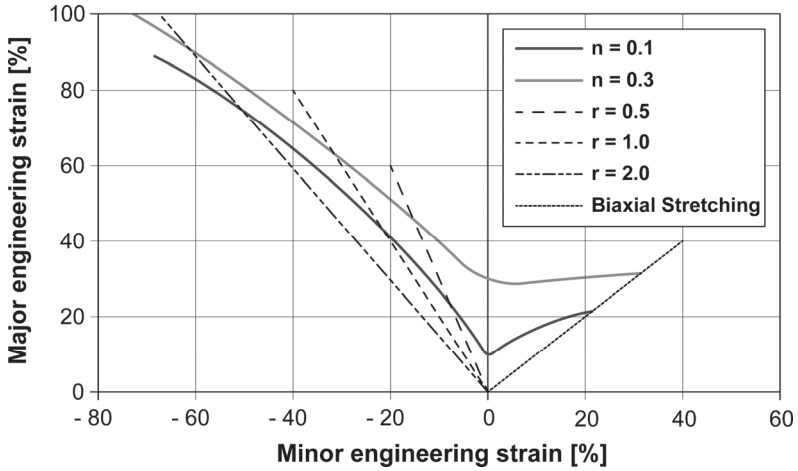

Figure 6: Influence of the normal anisotropy coefficient on the limit strains experimentally calculated using formulas number (6) and (7).

On the base of these observations, the evaluation of the ferritic stainless steels deformability and deep drawability requires further considerations. Referring to the tensile tests results reported in Figure 4, the percentage elongation of the ferritic stainless steels is about 2.5 times less than that of austenitic steels. Moreover, the ratio among the ferritic and austenitic steels strain energy (determined as the area under the tensile curves) is equal to about 1/3. On the other hand, the Erichsen index of the ferritic steels is about 1.3 times less than that of austenitic grades. Moreover, it must be remarked that the price of ferritic stainless steels is significantly lower (at least half) and more stable over time than that of austenitic one, which is strongly influenced by the cost of nickel. These observations suggest that the deep drawability of ferritic stainless steel can be significantly improved by working on new chemical compositions able to maximize the deformability, by a careful control of the production process aimed at increasing the normal anisotropy coefficient and, if possible, selecting slightly thicker sheets. S. K. Paul [19], in fact, reported an equation to calculate the major strain when the minor is zero (plain strain condition). This value, called FLD_0, can be predicted by Eqn. (8) when $n \leq 0.21$ and the thickness t is lower than 3.1 mm.

$$FLD_0 = \ln\left[1+\left(\frac{23.3+14.3t}{100}\right)\frac{n}{0.21}\right] \quad (8)$$

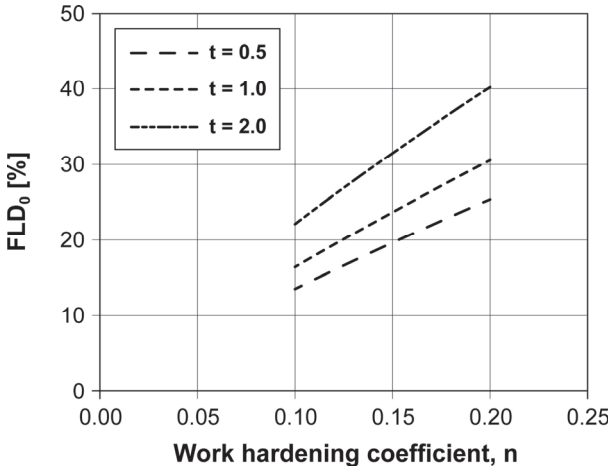

Figure 7: Influence of the strain hardening exponent and of the sheet thickness on the % FLD_0 value experimentally calculated using formula number (8).

Moreover, the lower cost justifies the choice of more effective, even though more expensive, technological parameters such as the punch speed and geometry, the blank-holder pressure and the lubricant type. All these factors affect the material deformability significantly as demonstrated by the data analysis shown in Figure 6 and Figure 7.

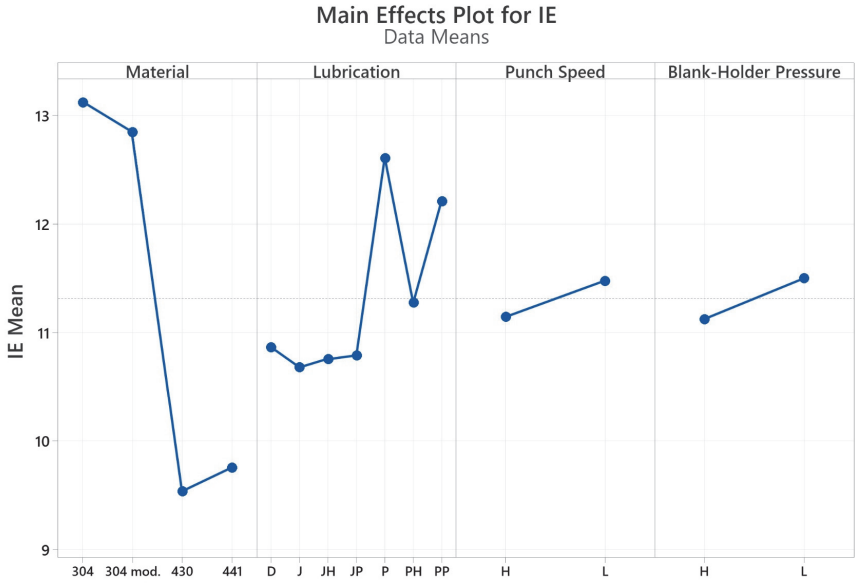

Figure 8: Effect of material, lubrication, punch speed and blank-holder pressure on the Erichsen index (IE). Preliminary visual analysis of the main factors (main effect plot).

Pairwise comparisons using the Tukey's test show that the PVC adhesive film significantly increases the Erichsen index, compared to tests performed without lubrication. In contrast, Petroleum jelly, a gelatinous lubricant, does not improve process performance, although it can reduce wear on machine components [5].
An explanation for the ineffectiveness of Petroleum jelly lies in the process conditions: high pressures tend to remove the viscous lubricant from the contact areas, preventing the reduction of the friction coefficient between the sheet metal and the punch or the blank-holder.
For PVC, it is observed that the lubricated area significantly affects the result. In particular, complete lubrication, i.e. of both areas in contact with the punch and the blank-holder, gives the best results, followed by lubrication of the punch only and

finally of the blank-holder only. Complete lubrication has two effects: it improves the sliding of the sheet metal in contact with the punch and increases the quantity of steel that flows in the area between the blank-holder and the punch. The most significant of the two effects is certainly the first, because the sliding of the sheet metal under the blank holder remains limited.

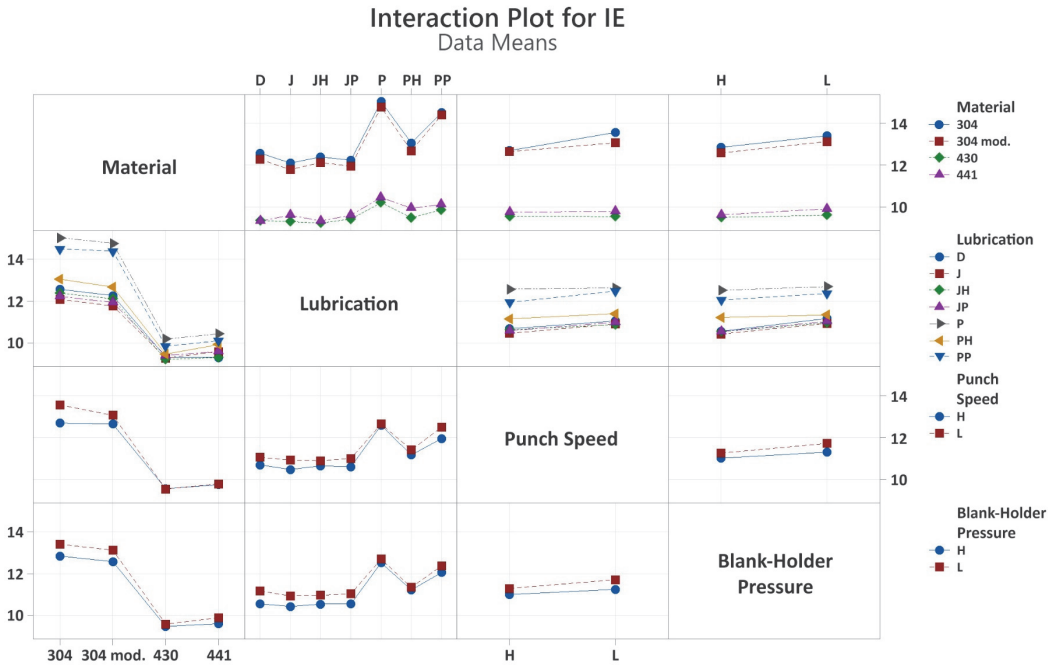

Figure 9: Effect of interactions between material, lubrication, punch speed and blank holder-pressure on the Erichsen index (IE). Preliminary visual analysis of interactions (Interaction Plot).

Source	DF	Adj SS	Adj MS	F-Value	P-Value
Material	3	941.48	313.826	5126.18	0.000
Lubrication	6	175.61	29.269	478.09	0.000
Punch Speed	1	9.10	9.101	148.67	0.000
Blank-Holder Pressure	1	11.93	11.925	194.79	0.000
Material*Lubrication	18	52.90	2.939	48.00	0.000
Material*Punch Speed	3	10.58	3.526	57.59	0.000
Material*Blank-Holder Pressure	3	2.98	0.993	16.23	0.000
Lubrication*Punch Speed	6	1.84	0.307	5.01	0.000
Lubrication*Blank-Holder Pressure	6	2.34	0.391	6.38	0.000
Punch Speed*Blank-Holder Pressure	1	0.64	0.643	10.51	0.001
Material*Lubrication*Punch Speed	18	2.54	0.141	2.31	0.003
Material*Lubrication*Blank-Holder Pressure	18	0.73	0.040	0.66	0.848
Material*Punch Speed*Blank-Holder Pressure	3	0.09	0.032	0.52	0.672
Lubrication*Punch Speed*Blank-Holder Pressure	6	1.16	0.193	3.15	0.005
Material*Lubrication*Punch Speed*Blank-Holder Pressure	18	1.07	0.060	0.97	0.490
Error	224	13.71	0.061		
Total	335	1228.71			

Table 6: ANOVA table of the main factors (material, lubrication, punch speed and blank-holder pressure) and their interactions up to the fourth order. In green the significant factors and interactions according to a p-value lower than 0.05.

As already observed for lubrication, the blank-holder pressure is also statistically significant, although it plays a minor role. In this case, a lower pressure is slightly more advantageous, since it improves the sliding of the sheet metal under the blank holder, feeding the deformation zone between the punch and the blank holder. This result confirms what has already been observed for lubrication: the more the sliding is promoted, the better the test results, since the greater the amount of stainless

steel that contributes to the deformation. It is in fact important to remark that the Erichsen test simulates the stretching conditions that can be present locally in deep drawing, such as, for example, the small radius areas nearby the die. In these cases, ensuring adequate sliding between the material and the die is essential for the success of the process, especially when the sheet metal is not completely blocked by the blank holder. Finally, it is important to highlight that the punch speed, and therefore the strain rate, also represents a statistically significant factor, although with a less relevant role than the stainless steel family and the lubrication.

Material	IE Mean	Grouping
304	13.1214	A
304 mod.	12.8476	B
441	9.7548	C
430	9.5369	D

Lubrication	IE Mean	Grouping
P	12.6083	A
PP	12.2125	B
PH	11.2813	C
D	10.8688	D
JP	10.7917	D E
JH	10.7583	D E
J	10.6854	E

Punch Speed	IE Mean	Grouping
L	11.4798	A
H	11.1506	B

Blank-Holder Pressure	IE Mean	Grouping
L	11.5036	A
H	11.1268	B

Material x Lubrication	IE Mean	Grouping
304 P	15.0333	A
304 mod. P	14.7667	A B
304 PP	14.5000	B C
304 mod. PP	14.3917	C
304 PH	13.0500	D
304 mod. PH	12.6750	E
304 D	12.5667	E F
304 JH	12.3833	E F G
304 mod. D	12.2667	F G H
304 JP	12.2250	F G H
304 mod. JH	12.1167	G H I
304 J	12.0917	G H I
304 mod. JP	11.9417	H I
304 mod. J	11.7750	I
441 P	10.4417	J
430 P	10.1917	J K
441 PP	10.1083	J K
441 PH	9.9250	K L
430 PP	9.8500	K L
441 J	9.5917	L M
441 JP	9.5917	L M
430 PH	9.4750	M N
430 JP	9.4083	M N
430 D	9.3333	M N
441 JH	9.3167	M N
441 D	9.3083	M N
430 J	9.2833	M N
430 JH	9.2167	N

Material x Punch Speed	IE Mean	Grouping
304 L	13.5571	A
304 mod. L	13.0571	B
304 H	12.6857	C
304 mod. H	12.6381	C
441 L	9.7762	D
441 H	9.7333	D
430 H	9.5452	E
430 L	9.5286	E

Lubrication x Blank-Holder Pressure	IE Mean	Grouping
P L	12.6958	A
P H	12.5208	A B
PP L	12.3708	B
PP H	12.0542	C
PH L	11.3417	D
PH H	11.2208	D E
D L	11.1750	D E F
JP L	11.0333	E F
JH L	10.9708	F
J L	10.9375	F
D H	10.5625	G
JP H	10.5500	G
JH H	10.5458	G
J H	10.4333	G

Lubrication x Punch Speed	IE Mean	Grouping
P L	12.6375	A
P H	12.5792	A
PP L	12.4833	A
PP H	11.9417	B
PH L	11.4042	C
PH H	11.1583	D
D L	11.0542	D E
JP L	10.9917	D E
J L	10.9083	E F
JH L	10.8792	E F
D H	10.6833	F G
JH H	10.6375	G
JP H	10.5917	G
J H	10.4625	G

Punch Speed x Blank-Holder Pressure	Mean	Grouping
L L	11.7119	A
H L	11.2952	B
L H	11.2476	B
H H	11.0060	C

Material x Blank-Holder Pressure	Mean	Grouping
304 L	13.4024	A
304 mod. L	13.1214	B
304 H	12.8405	C
304 mod. H	12.5738	D
441 L	9.8976	E
441 H	9.6119	F
430 L	9.5929	F
430 H	9.4810	F

Table 7: Multiple comparisons according to Tukey's test (p-value equal to 0.05) between the factor levels and their interactions up to the second order. Each statistically different factor and interaction is indicated by a different letter. (Example 1: Pairwise comparison between materials shows that all four stainless steels exhibit statistically different IE; Example 2: Pairwise comparison between lubrication methods shows that, in terms of IE, PVC lubrication on both the punch and the blank holder (group A), on the punch only (group B), and on the blank holder only (group C) are statistically different from each other and also from the condition without lubrication (group D) and from all those with petroleum Jelly (groups D and E). The conditions without lubrication (group D) and all those with Petroleum Jelly (group E) are statistically equal to each other.

Pairwise comparisons using the Tukey's test demonstrate that a lower punch speed improves the Erichsen index, since it makes the dislocation motion easier [25]. The difference between the levels appears limited, despite the two extreme conditions chosen for the tests (4.3 mm/min and 120 mm/min). At room temperature, the load rate has a significant influence only when it is very high ($\dot{\varepsilon} > 100$ 1/s), such as in high-velocity ballistic impacts [8–10].

Regarding the interactions between factors, it is important to highlight that ferritic stainless steels always show lower performance than austenitic ones, regardless of lubrication conditions, punch speed and blank-holder pressure. At the same time, however, ferritic stainless steels are less sensitive to these three factors than austenitic ones. The maximum percentage difference between the best and worst lubrication conditions for ferritic stainless steels is about 10.7%, compared to about 21.7% for austenitic ones. The same trend is also observed for punch speed and blank-holder pressure, which show a maximum percentage difference of 2.5% and 4.2% for ferritic stainless steels compared to 6.8% and 6.2% for austenitic ones, respectively. This difference demonstrates that to take full advantage of the large cold plastic deformation of stainless steels it is very important to use process parameters that improve their flow.

Metallographic analysis

Chemical analyses, tensile tests and Erichsen tests shown very limited differences between the standard grades (AISI 304 and AISI 430) and the ones with improved deep drawability (304 mod. and AISI 441). For this reason, metallographic analyses and HV0.2 microhardness tests were carried out only on the former, which are more commonly used in industrial processes. Regarding the lubricant type, it was decided to limit the analyses to two experimental conditions: (i) with PVC film on the punch and the blank holder area and (ii) without lubrication. The materials tested with petroleum jelly were not investigated for the limited effects observed in the Erichsen tests. For the punch speed and the blank-holder pressure, the

low values (4.3 mm/min and 6.6 MPa respectively) cases were selected, since they resulted in better Erichsen indexes. Metallographic analyses were performed at two magnifications, 5x and 100x, in order to describe the microstructure from both general (Figure 10) and detailed (Figure 11) points of view, in correspondence with the areas listed below.

- Area A: under the blank-holder.
- Area B: near the knee, just beyond the blank-holder.
- Area C: between the punch and blank-holder.
- Areas D, E and F: characterized by a strong thinning and/or localized necking of the sheet metal. Depending on material and lubrication, these areas are located in the non-contact zone between the punch and the blank holder or in the spherical cup.

The results were presented starting from the austenitic stainless steel AISI 304, first without lubrication and then with the use of PVC film. The same procedure was also applied to the ferritic stainless steel AISI 430. The zone A of the AISI 304, below the blank-holder, shows almost equiaxed grains typical of the sheet metal in the solubilized state. The microstructure confirms that the plastic flow is extremely limited in this zone. Zones B, C and E instead show an opposite situation, with grains strongly elongated along the deformation direction. In these areas, the microstructure is influenced by the load conditions generated by the Erichsen test, i.e. a strong stretching between the punch and the blank-holder. Zones D and F are of extreme interest, since the amount of plastic deformation strongly depends on the lubrication method. Without lubrication, zone F has a very little deformation, because the high friction contrasts the sliding of the sheet metal; this condition also influences zone D which undergoes localized necking phenomena. This area is in fact located approximately halfway between the blank-holder and the top of the cup, where the sheet metal is almost constrained in its movements. The use of the PVC film lubricant completely changes the operating conditions, allowing the sheet metal to slide and spread the plastic deformation between the C and F zones. The images reported in Figure 10 and Figure 11 show a constant reduction in thickness, without highlighting the localized necking generated without lubrication. The strong influence of lubrication on the ability to spread the deformations is also confirmed by AISI 430, which shows the same features highlighted by AISI 304, compared to which, however, it shows a more limited plastic deformation.

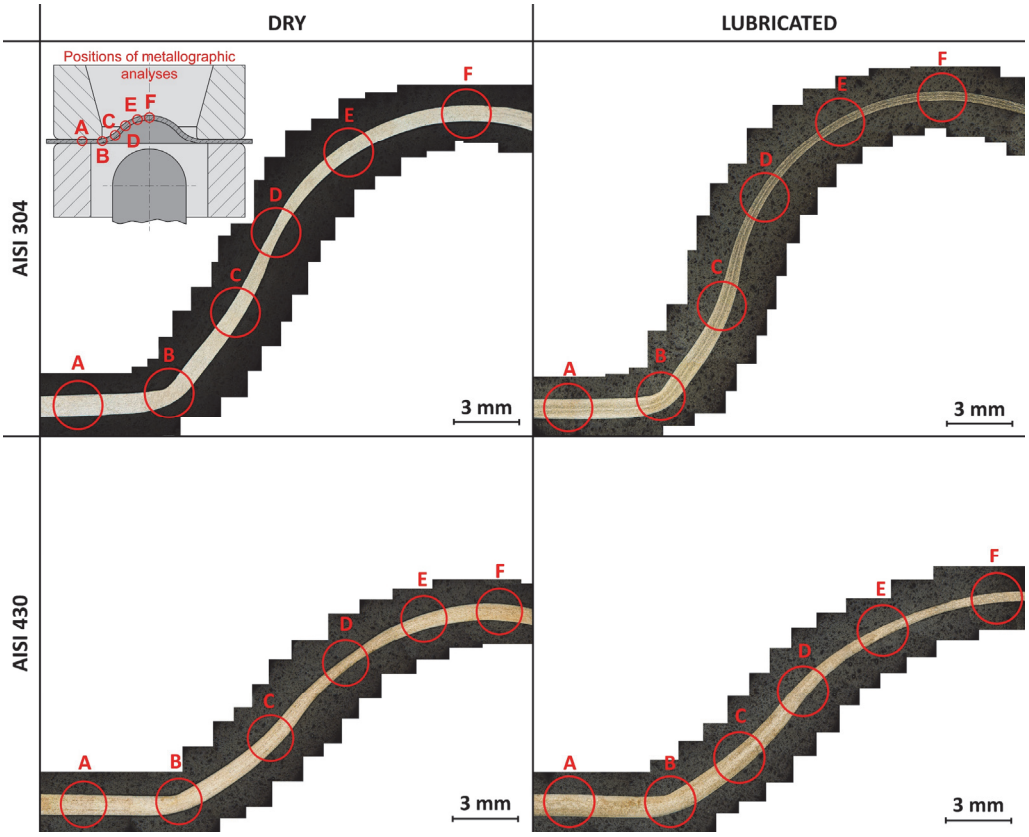

Figure 10: Metallographic analyses at low magnification after the Erichsen tests (5x): the letters from A to E highlights the areas analysed at 100x, summarised in Figure 11. For AISI 430 and AISI 441 the etching was carried out by immersion in a solution of 5 mL of hydrochloric acid and 1 g of picric acid in 100 mL of ethanol. For AISI 304 and 304 mod. the etching was carried out electrochemically with a solution of 10 g of oxalic acid in 100 mL of distilled water.

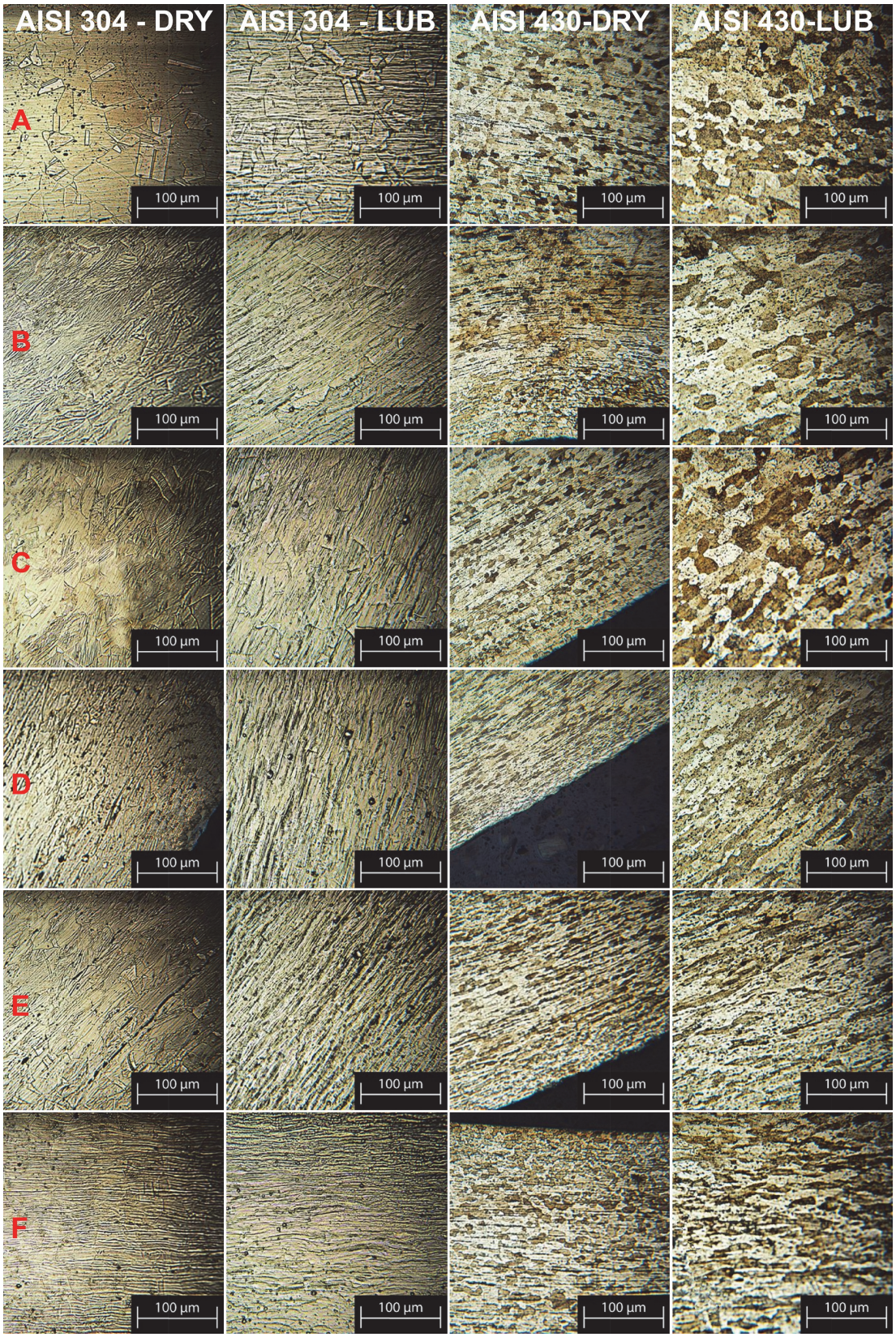

Figure 11: Metallographic analyses at 100x after the Erichsen test of the areas from A to E indicated in Figure 10. The DRY conditions were without lubrication while the LUB conditions were with PVC film in the punch and blank-holder areas. In both cases the punch speed and the blank-holder pressure were set at 4.3 mm/min and 6.6 MPa. For AISI 430 and AISI 441 the chemical etching was carried out by immersion in a solution of 5 mL of hydrochloric acid and 1 g of picric acid in 100 mL of ethanol. For AISI 304 and 304 mod. the chemical etching was carried out electrochemically with a solution of 10 g of oxalic acid in 100 mL of distilled water.

Hardness tests

The metallographic samples were also used to evaluate the HV0.2 (0.2 kg_f, 15 s) Vickers microhardness according to standard ISO 6507. The tests were performed on ten different areas, shown in Figure 12, in order to characterize the hardness on the Erichsen samples for both the stainless steel types (AISI 304 and AISI 430) and the lubrication methods (without lubrication and with PVC film). For each area, the hardness was evaluated near the inner and outer edge of the sheet metal and at half of its effective thickness. Specifically, areas 1 and 2 refer to the stainless steel under the blank-holder, areas 3 and 4 are located near the knee just beyond the blank-holder, while areas 5, 6 and 7 are located in the contact-free area between the blank-holder and the punch. Areas 8, 9 and 10 are instead representative of the spherical cup produced by the punch.

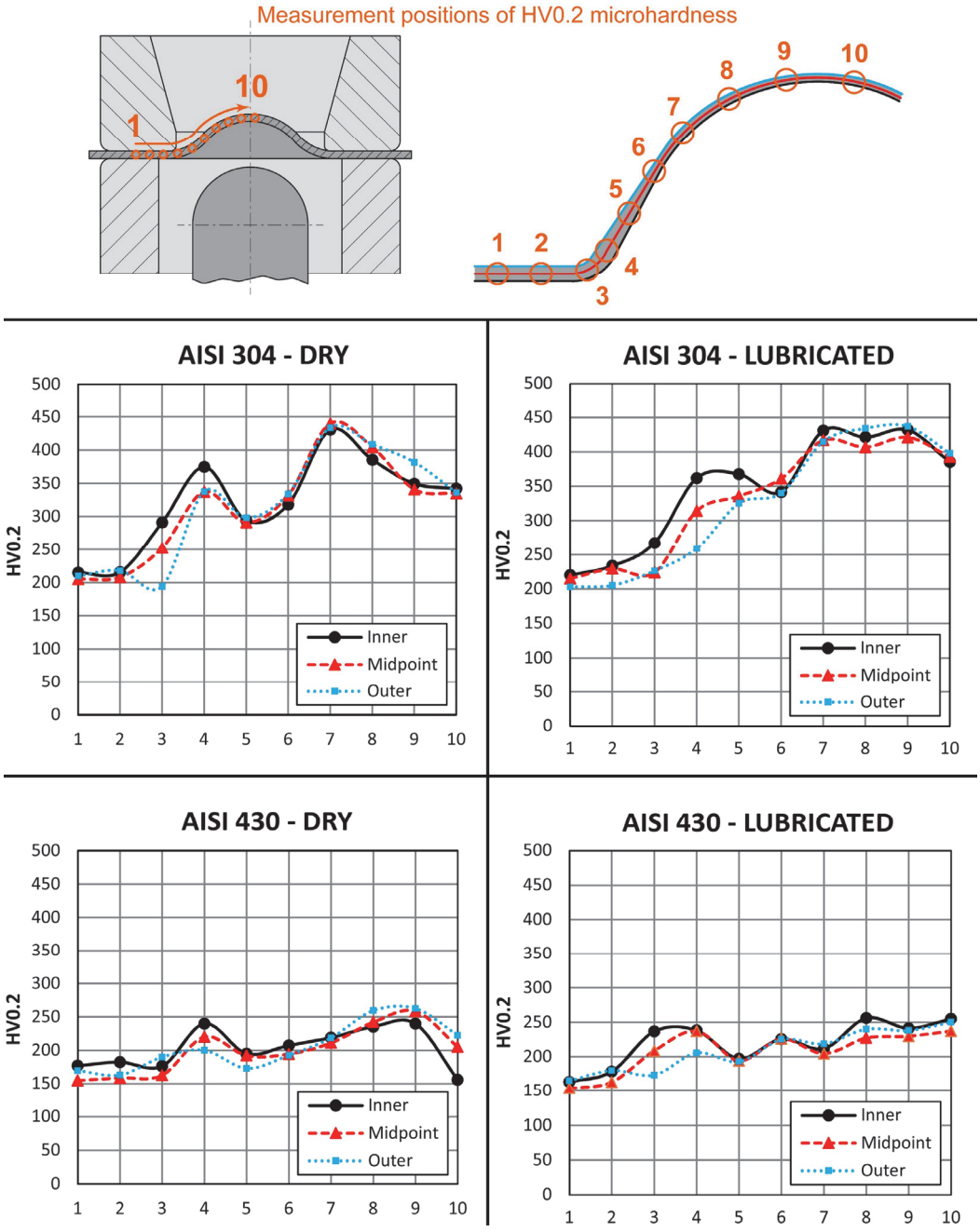

Figure 12: HV0.2 microhardness profiles along the Erichsen samples (areas 1 to 10) already used for metallographic analyses. The DRY conditions were obtained without lubrication, while the LUBRICATED conditions were obtained by applying the PVC film in the punch and blank holder areas. In both cases, the punch speed and the blank holder pressure were set equal to 4.3 mm/min and 6.6 MPa respectively.

The results, summarized in Figure 12, confirm that AISI 304 has a significantly higher work hardening in respect to AISI 430. The former, in fact, shows Vickers HV0.2 microhardness values up to 180 points higher than the latter in the areas of highest plastic deformation. In zones 1 and 2, below the blank holder, the hardness is consistent with the solubilized state before plastic deformation, highlighting very limited plastic flow. Zones 3 and 4 show a hardness increase due to the plastic deformation of the sheet metal, forced to bend around the radius of the die. In these areas, the hardness just below the inner edge is higher than that on the outer edge and in the half-thickness plane. In fact, in zones 3 and 4, the inner edge is opposite to the die and is therefore subject to maximum deformations. In areas 5 to 10, the hardness level is strongly influenced by the lubrication methods. The use of the PVC film lubricant allows the sheet metal to slide and distribute the plastic deformation uniformly both in the area between the blank-holder and the punch and below the latter; the hardness values therefore increase and reach their maximum at the apex of the spherical cup. Without lubrication, the high friction between the punch and the sheet metal counteracts the sliding at the apex of the spherical cup, where the deformation is very little and the sheets is characterised by hardness levels up to 100 HV0.2 points lower than those of lubricated ones. Without lubrication, the maximum hardness value is therefore in zone 7, approximately halfway between the blank-holder and the apex of the cup, which undergoes localized necking phenomena.

Conclusion

This research paper compares the performances of austenitic and ferritic stainless steels improved for deep drawing, 304 mod. and AISI 441, with the standard AISI 304 and AISI 430 grades. For all steels, the chemical composition, the mechanical properties (R_m, $R_{p0.2}$, A_g%, A%, n and r) and the Erichsen index (IE) were systematically evaluated in order to understand the effect of the main process parameters (lubrication, punch speed and blank-holder pressure) and their interactions on the deep drawing process. Some of the specimens used for the Erichsen tests were subjected to metallographic analyses and HV0.2 microhardness tests to study the modification of the microstructure during the test and its effect on local mechanical properties. The experimental plan was designed following the Design of Experiment (DoE) for complete and orthogonal plans replicated three times, while the results were statistically analysed with the ANOVA technique, that maximizes the effectiveness of the experiment. The results allow to draw the following conclusions.

- The tensile tests show no significant differences between the standard stainless steel grades (AISI 304 and AISI 430) and the ones with improved formability (304 mod. and AISI 441). Regarding the Erichsen tests, the austenitic grades showed very similar behaviour, whereas AISI 441 resulted in a limited increase of the Erichsen index. Even if AISI 430 and 441 grades showed similar formability and tensile properties, it must be remarked the higher PREN number of the latter, that can make it a better choice when superior corrosion resistance is required. Comparing austenitic and ferritic grades, the test results confirm the expected mechanical properties and formability differences: the yield strength of ferritic stainless steels is higher than that of austenitic ones which, however, have higher ultimate tensile strength because of the higher strain hardening exponent. This combination of properties allows austenitic stainless steels to achieve greater Erichsen index and to limit necking phenomena. Even if the gap among their formability can hardly be zeroed, it can be reduced working on the ferritic steels microstructural texture in order to increase the strain hardening exponent. Moreover, the significant lower cost justifies further research on the chemical composition and the selection of process parameters, such as the lubricant type, the punch speed and geometry, the blank-holder pressure and the sheet thickness, able to enhance the formability even when they are more expensive than those used for austenitic grades.
- PVC film lubricant significantly increases the Erichsen Index compared to unlubricated processes. In contrast, petroleum jelly, a gel-like lubricant, does not improve the process performance. This is because high pressures tend to move away petroleum jelly from contact areas, preventing effective friction reduction between the sheet metal and the punch or blank holder.
- The dimension of the lubricated zone influences the outcome of the Erichsen test. Complete lubrication (punch and blank-holder) ensures optimum results. The next most effective lubrication methods are, in decreasing order of effectiveness, lubrication of the punch only and, subsequently, of the blank holder only. Complete lubrication promotes both the sliding of the sheet metal over the punch and the increase in material flow between the blank holder and the punch. The first effect is the most significant, since the sliding capacity under the blank holder is limited in any case.
- Both the blank-holder pressure and the punch speed are technically and statistically significant factors, although with a lower influence than the stainless steel family and their lubrication. A lower blank-holder pressure is slightly more advantageous, as it makes the sliding of the sheet metal easier and improves the feeding of the area between

the blank-holder and the punch. Similarly, lower punch speeds improve the Erichsen index, facilitating the dislocation motion.

- The interactions between factors show that ferritic stainless steels perform worse than austenitic ones, regardless of lubrication, punch speed and blank-holder pressure. However, ferritic stainless steels show a lower sensitivity to these three factors. This difference highlights how, in order to maximize the plastic deformation of stainless steels, it is essential to optimize the process parameters that improve their flow. This characteristic is more evident in austenitic stainless steels, given their superior plastic deformation capacity compared to ferritic ones. They, in fact, exhibit significantly greater work hardening. In particular, austenitic stainless steels show Vickers HV0.2 microhardness values up to 180 points higher in the areas of maximum plastic deformation.
- Metallographic analyses and hardness tests reveal that lubrication methods have a huge influence on work hardening and local mechanical properties. Lubrication with PVC film promotes uniform plastic deformation between the blank holder and the punch, and below the punch, resulting in higher hardness values that peak at the apex of the spherical cup. On the contrary, the absence of lubrication results in high friction, counteracting sliding at the apex and leading to minimum deformation and hardness values, up to 100 HV0.2 points lower than lubricated sheets in that area. Without lubrication, the maximum work hardening and, therefore the highest hardness, moves approximately halfway between the blank holder and the apex of the cup, where localized necking occurs.

REFERENCES

[1] Casaroli, A., Boniardi, M., Gerosa, R., Bilo, F., Borgese, L., Cirelli, P., Depero, L.E. (2022). Metals release from stainless steel knives in simulated food contact, Food Addit Contam Part B Surveill, 15(3), pp. 203–211. DOI: https://doi.org/10.1080/19393210.2022.2075473.

[2] Casaroli, A., Boniardi, M., Dalipi, R., Borgese, L., Depero, L.E. (2021). Procedure optimization of type 304 and 420B stainless steels release in acetic acid, Food Control, 120. DOI: https://doi.org/10.1016/j.foodcont.2020.107509.

[3] Tiwari, P.R., Rathore, A., Bodkhe, M.G. (2022). Factors affecting the deep drawing process – A review, Mater Today Proc, 56, pp. 2902–2908. DOI: https://doi.org/10.1016/j.matpr.2021.10.189.

[4] Yang, T.S. (2010). Investigation of the strain distribution with lubrication during the deep drawing process, Tribol Int, 43(5–6), pp. 1104–1112. DOI: https://doi.org/10.1016/j.triboint.2009.12.050.

[5] Boher, C., Attaf, D., Penazzi, L., Levaillant, C. (2005). Wear behaviour on the radius portion of a die in deep-drawing: Identification, localisation and evolution of the surface damage, Wear, 259(7–12), pp. 1097–1108. DOI: https://doi.org/10.1016/j.wear.2005.02.101.

[6] Chen, D., Zhao, C., Chen, X., Li, H., Zhang, X. (2022). Research on the active pressurized forced lubrication deep drawing process and evaluation of the lubrication effect, International Journal of Advanced Manufacturing Technology, 120(3–4), pp. 2815–2826. DOI: https://doi.org/10.1007/s00170-022-08892-z.

[7] Singer, M., Liewald, M. (2014). Effect of surface enlargement and of viscosity of lubricants on friction behaviour of advanced high strength steel material during deep drawing., Advanced Materials Research, 1018, pp. 253–260.

[8] Andreotti, R., Casaroli, A., Colamartino, I., Quercia, M., Boniardi, M.V., Berto, F. (2023). Ballistic Impacts with Bullet Splash—Load History Estimation for.308 Bullets vs. Hard Steel Targets, Materials, 16(11). DOI: https://doi.org/10.3390/ma16113990.

[9] Andreotti, R., Abate, S., Casaroli, A., Quercia, M., Fossati, R., Boniardi, M. V. (2021). A simplified ale model for finite element simulation of ballistic impacts with bullet splash – development and experimental validation, Frattura Ed Integrita Strutturale, 15(57), pp. 223–245. DOI: https://doi.org/10.3221/IGF-ESIS.57.17.

[10] Andreotti, R., Quercia, M., Casaroli, A., Boniardi, M. V. (2023). Load history estimation for ballistic impacts with bullet-splash., Procedia Structural Integrity, 51, pp. 37–43.

[11] Dewang, Y., Sharma, V., Batham, Y. (2021). Influence of Punch Velocity on Deformation Behavior in Deep Drawing of Aluminum Alloy, Journal of Failure Analysis and Prevention, 21(2), pp. 472–487. DOI: https://doi.org/10.1007/s11668-020-01084-5.

[12] Choi, J.-Y., Jin, W. (1997). Strain induced martensite formation and its effect on strain hardening behavior in the cold drawn 304 austenitic stainless steels, 36.

[13] Nohara, K., Ono, Y., Ohashi, N. (1977). Composition and grain size dependencies of strain-induced martensitic transformation in metastable Austenitic stainless steels, 63, pp. 772–782. DOI: https://doi.org/10.2355/tetsutohagane1955.63.5_772.

[14] Ishimaru, E., Hamasaki, H., Yoshida, F. (2014). Deformation-induced martensitic transformation and workhardening of type 304 stainless steel sheet during draw-bending., Procedia Engineering, 81, pp. 921–926.
[15] Cashell, K.A., Baddoo, N.R. (2014). Ferritic stainless steels in structural applications, Thin-Walled Structures, 83, pp. 169–181. DOI: https://doi.org/10.1016/j.tws.2014.03.014.
[16] Semiantin, S.L. (2006). ASM Handbook, Volume 14b: Metalworking: Sheet Forming, ASM International.
[17] Wang, L., Lee, T.C. (2006). The effect of yield criteria on the forming limit curve prediction and the deep drawing process simulation, Int J Mach Tools Manuf, 46(9), pp. 988–995. DOI: https://doi.org/10.1016/j.ijmachtools.2005.07.050.
[18] Jaamialahmadi, A., Kadkhodayan, M. (2012). A modified Storen-Rice bifurcation analysis of sheet metal forming limit diagrams, Journal of Applied Mechanics, Transactions ASME, 79(6). DOI: https://doi.org/10.1115/1.4005538.
[19] Paul, S.K. (2021). Controlling factors of forming limit curve: A review, Advances in Industrial and Manufacturing Engineering. DOI: https://doi.org/10.1016/j.aime.2021.100033.
[20] Paul, S.K. (2013). Theoretical analysis of strain- and stress-based forming limit diagrams, Journal of Strain Analysis for Engineering Design, 48(3), pp. 177–188. DOI: https://doi.org/10.1177/0309324712468524.
[21] Forming Limit Diagram (FLD) for sheet metal forming applications. (n.d.).
[22] Okayasu, M., Ishida, D. (2019). Effect of Microstructural Characteristics on Mechanical Properties of Austenitic, Ferritic, and γ-α Duplex Stainless Steels, Metall Mater Trans A Phys Metall Mater Sci, 50(3), pp. 1380–1388. DOI: https://doi.org/10.1007/s11661-018-5083-4.
[23] Montgomery, D.C. (2013). Design and analysis of experiments, John Wiley & Sons, Inc.
[24] Storen, S., Rice, J.R. (1975). Localized necking in thin sheets, 23, Pergamon Press.
[25] Clyne, T.W., Campbell, J.E. (2021). Testing of the Plastic Deformation of Metals, Cambridge University Press.